

Recession flow analysis for aquifer parameter determination

Jozsef Szilagyi

Conservation and Survey Division, University of Nebraska, Lincoln

Marc B. Parlange

Department of Geography and Environmental Engineering, Johns Hopkins University, Baltimore, Maryland

John D. Albertson

Department of Environmental Sciences, University of Virginia, Charlottesville

Abstract. The recession flow analysis of *Brutsaert and Nieber* [1977] extended by *Troch et al.* [1993] to estimate aquifer parameters (saturated hydraulic conductivity and mean aquifer depth) is examined by means of a numerical model. It is found to be reliable for the estimation of the catchment-scale saturated hydraulic conductivity and mean aquifer depth. Increasing the complexity of the synthetic watershed had no impact on the accuracy of the estimated parameters.

1. Introduction

Brutsaert and Nieber [1977] presented a technique for the estimation of the aquifer-scale saturated hydraulic conductivity k which was extended by *Troch et al.* [1993] also to estimate the mean aquifer depth D . The method utilizes streamflow recession hydrographs and some basic geomorphological properties of the watershed (i.e., the total length of the streams and the catchment area). The analysis is based on analytical solutions of the one-dimensional Boussinesq equation describing the transient behavior of an unconfined groundwater body under Dupuit's assumption (i.e., the hydraulic head is independent of depth). A detailed description of the technique can be found in the above-mentioned references. Below we briefly outline the steps involved.

The Boussinesq equation, when the effect of capillarity above the water table is neglected and the Dupuit approximation is invoked, describes the elevation of the transient groundwater table $h(x, t)$ above a horizontal impermeable layer

$$\frac{\partial h}{\partial t} = \frac{k}{\varphi} \frac{\partial}{\partial x} \left(h \frac{\partial h}{\partial x} \right) \quad (1)$$

where k is the (constant) saturated hydraulic conductivity of the unconfined aquifer, φ is the (constant) drainable porosity, t is time, and x is horizontal distance. See Figure 1 for a schematic cross section of this system. For a so-called fully penetrating stream draining an initially saturated aquifer of finite width B , there exists an analytical short-time solution to (1) [see *Polubarinova-Kochina*, 1962, p. 507] when the groundwater drainage is not yet influenced by the no-flow condition at the edge of the aquifer. The resulting outflow rate (per unit length) to the channel is [Polubarinova-Kochina, 1962, p. 507]

$$q(t) = 0.332(k\varphi)^{1/2}D^{3/2}t^{-1/2} \quad (2)$$

where D is the aquifer depth and t is time. When the recession drawdown reaches the entire breadth of the aquifer (i.e., at time t_3 in Figure 1, where $h(x, t) < D$, everywhere), the long-time

solution becomes valid, reflecting the effect of the no-flow boundary on the groundwater drainage [see *Polubarinova-Kochina*, 1962, p. 515–517]. The outflow rate for the long-time solution can be expressed, as was first shown by *Boussinesq* [1903] and later by *Polubarinova-Kochina* [1962, p. 517]

$$q(t') = \frac{0.862kD^2}{B \left[1 + 1.115 \left(\frac{kD}{\varphi B^2} \right) t' \right]^2} \quad (3)$$

where B is the width of the aquifer and t' is time with an origin outside of the short-time solution range. The two equations for the short- and long-time outflow rate contain the four parameters φ , k , D , and B . Therefore, with observations of streamflow versus time and a priori estimates of any two of these parameters the equations can be inverted to provide estimates of the remaining two parameters. For example, if the values of φ and B were known, k and D could be estimated with use of measured discharges at the outlet of the catchment. Equally, one could choose to prescribe k on the basis of knowledge of the aquifer material instead of φ , but since the value of k may range over some 11 orders of magnitude while the range for φ is only one order of magnitude [Domenico and Schwartz, 1998, pp. 15 and 39] it is more useful to prescribe φ [Anderson and Woessner, 1992, p. 69]. Employing the definition of the drainage density [Horton, 1945] $R_d (=LA^{-1}$, where L is the total length of the contributing streams and A is the area of the watershed) an effective value of B can be obtained as $B = (2R_d)^{-1}$ for natural watersheds. The value of φ can be estimated from available tables on the basis of knowledge of the type of aquifer material.

The last obstacle before the direct application of the outflow rate solutions for estimating k and D is the determination of the time origin (i.e., the time when groundwater drawdown begins). However, this is not generally known, so *Brutsaert and Nieber* [1977] suggested that one should analyze the slope of the hydrograph (dQ/dt) as a function of the discharge Q . For both the short- and the long-time solutions for the outflow rate the slope of the hydrograph can be expressed as

$$\frac{dQ}{dt} = -aQ^b \quad (4)$$

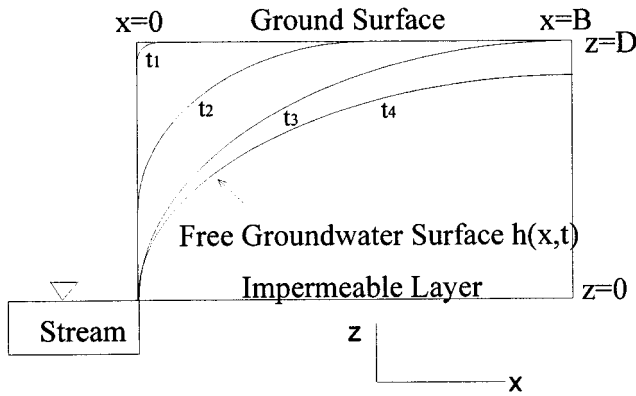


Figure 1. Schematic diagram of an unconfined aquifer with a fully penetrating stream. The shape of the free groundwater surface is shown through time following saturation of the aquifer.

where $Q(t)$ is the measured discharge and a and b are constants [Brutsaert and Nieber, 1977]. From the solutions for the outflow rate and appropriate expressions for R_d and B the constants in (4) can be related back to the above mentioned four parameters (φ , k , D , and B) as

$$a_1 = \frac{4.532B^2}{k\varphi D^3 A^2} \quad b_1 = 3 \quad (5)$$

for the short-time solution, and

$$a_2 = \frac{4.804k^{1/2}L}{\varphi A^{3/2}} \quad b_2 = \frac{3}{2} \quad (6)$$

for the long-time solution [Brutsaert and Nieber, 1977; Troch et al., 1993]. Equation (4) plotted as $\log(-dQ/dt)$ versus $\log(Q)$ forms straight lines with slopes of 3 for the short-time and 1.5 for the long-time solutions with corresponding intercepts a_1 and a_2 , respectively.

When applying baseflow recession techniques in practice for estimating aquifer parameters, it is very hard to check the accuracy of the estimated values since, generally, they are not known for heterogeneous systems such as watersheds. Moreover, when estimating the catchment-scale hydraulic conductivity by the Brutsaert-Nieber technique, the resulting values are generally 1–2 magnitudes larger than their laboratory-derived counterparts [Troch et al., 1993]. This is because the catchment-scale estimate incorporates the effect of preferential flow, flow in macropores [Troch et al., 1993], and the possible high spatial autocorrelation of the conductivity values in certain directions. By employing a numerical model for the simulation of catchment behavior based on the numerical integration of the two-dimensional Boussinesq equation we are in a position to control the parameters characteristic of the watershed. Consequently, the baseflow recession estimates of the catchment-scale parameters can readily be evaluated. This type of comparison has not been performed for the Brutsaert-Nieber recession flow technique, which motivated the present work.

In this paper we investigate the performance of the Brutsaert-Nieber [1977] recession flow analysis for aquifer-scale parameter (k and D) estimation using a numerical model when the conditions required for the technique (i.e., the Dupuit approximation is applicable where a fully incised stream drains an initially saturated aquifer and where any effect of capillarity on the groundwater drainage is negligible) are met. The focus

Table 1. Prescribed Parameters of the Aquifers Used in the Numerical Model and Their Estimated Values Using the Recession Flow Technique

| | Rectangularly Shaped Aquifer | | Synthetic Watershed | |
|---|--|--|---|--|
| | Prescribed | Estimated | Prescribed | Estimated |
| a/constant k | $D = 10, B = 400, L = 100, \text{ and } \varphi = 0.1$ $k = 10^{-4}$ | $k_{\text{est}} = 1.09 \times 10^{-4}$ and $D_{\text{est}} = 9.61$ | $D = 10, A = 5.762 \times 10^5, L = 1.49 \times 10^3, R_d = 2.58 \times 10^{-3},$ $B = 193.35, \text{ and } \varphi = 0.1$ | $k_{\text{est}} = 6.00 \times 10^{-5}$ and $D_{\text{est}} = 8.57$ |
| b/spatially variable k | $\text{pdf}(k) = \psi(\alpha, \beta, \gamma), \alpha = \exp(\gamma\gamma + \beta),$ $\gamma = N(0, 1), \beta = -9.6, \gamma = 2, n = 400,$ $\langle k \rangle = 8.21 \times 10^{-4}, \langle k_{\varphi} \rangle = 0.91 \times 10^{-4},$ $k_{\text{max}} = 0.0984, k_{\text{min}} = 3.22 \times 10^{-7},$ and $k_{\text{mod}} = 0.90 \times 10^{-4}$ Same as $b/$ | $k_{\text{est}} = 1.36 \times 10^{-4}$ and $D_{\text{est}} = 10.00$ | $\text{pdf}(k) = \psi(\alpha, \beta, \gamma), \alpha = \exp(\gamma\gamma + \beta), \gamma = N(0, 1), \beta = -9.6,$ $\gamma = 2, n = 5762, \langle k \rangle = 5.63 \times 10^{-4}, \langle k_{\varphi} \rangle = 6.99 \times 10^{-5},$ $k_{\text{max}} = 0.417, k_{\text{min}} = 2.12 \times 10^{-8}, \text{ and } k_{\text{mod}} = 6.99 \times 10^{-5}$ | $k_{\text{est}} = 4.76 \times 10^{-5}$ and $D_{\text{est}} = 10.00$ |
| c/spatially variable k with preferred directions | Same as $b/$ | $k_{\text{est}} = 5.52 \times 10^{-4}$ and $D_{\text{est}} = 7.96$ | same as $b/$ | $k_{\text{est}} = 4.12 \times 10^{-5}$ and $D_{\text{est}} = 9.54$ |
| d/constant k with sloping impervious layer | $k = 10^{-4}, \text{ slope} = 1:100, \text{ and } D = 8;$ see Figure 6 | $k_{\text{est}} = 1.17 \times 10^{-4}$ and $D_{\text{est}} = 8.80$ | not investigated | not investigated |
| e/spatially variable k , sloping impervious layer | same as $b/$ with a slope same as $d/$ and $D = 8$ | $k_{\text{est}} = 1.42 \times 10^{-4}$ and $D_{\text{est}} = 9.23$ | same as $b/$; for slope conditions see Figure 6; $D = 8$ | $k_{\text{est}} = 5.64 \times 10^{-5}$ and $D_{\text{est}} = 8.65$ |

B , aquifer width (meters); D and D_{est} , mean aquifer depth (meters) and its estimated value; φ , drainable porosity; k and k_{est} , saturated hydraulic conductivity (ms^{-1}) and its estimated value; $\langle k \rangle$ and $\langle k_{\varphi} \rangle$, arithmetic and geometric average of k ; k_{min} , k_{max} , and k_{mod} , minimum, maximum, and mode of the generated and lognormally distributed saturated hydraulic conductivities; L , channel length (meters); n , number of cells applied in the numerical model; $\text{pdf}(k)$, probability density function (given by $\psi(\alpha, \beta, \gamma)$, where β, γ are the parameters of the lognormal distribution) of the generated saturated hydraulic conductivities; R_d , drainage density (per meter); and γ , computer-generated value with a standard normal distribution.

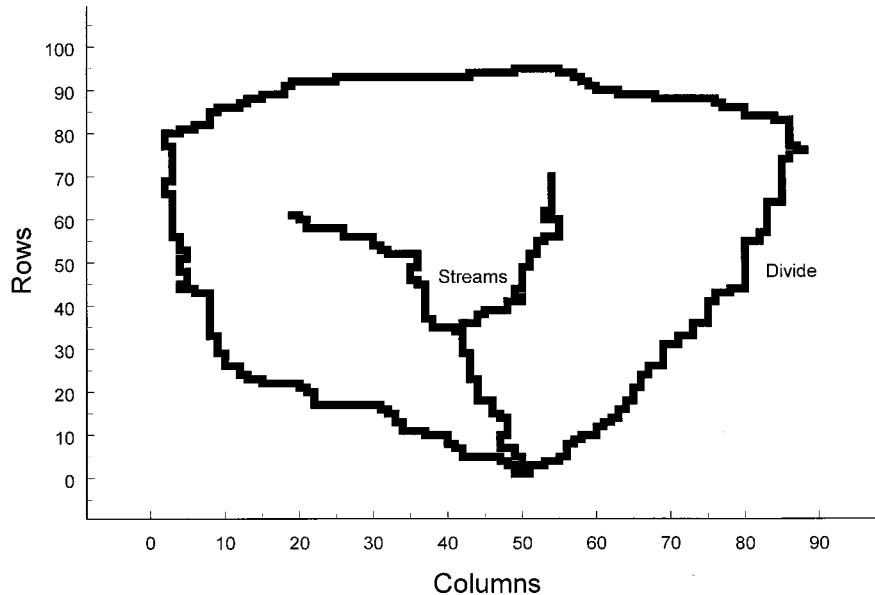


Figure 2. The geometry of the synthetic catchment. Cell dimensions are 10 by 10 m.

of our work is to check how the complex shape of a watershed, heterogeneity of hydraulic conductivity, and a gently sloping impermeable layer influence the estimated parameters.

2. Parameter Reliability Test

We test the robustness of the *Brutsaert-Nieber* [1977] recession flow analysis for estimating two catchment-scale parameters (k and D) by comparison of the estimated parameters to prescribed values employed in a numerical model. The analysis is carried out in two stages. Since the analytical solution of the 1-D Boussinesq equation is strictly valid only for a rectangular region we first model the transient unconfined groundwater profile in a rectangularly shaped aquifer. The effect of spatial variability of the saturated hydraulic conductivities, as well as macroscopic anisotropy (i.e., high spatial autocorrelation in certain directions), on the estimated catchment-scale parameters is checked. Similarly, we test the effect of a gently sloping impervious layer (when the Dupuit assumption can still be applied) on the estimated watershed parameters. In the second stage of analysis the above tests were repeated for a small synthetic (nonrectangular) catchment with an area A of 576,200 m².

In both cases the behavior of the transient unconfined groundwater profile was simulated by numerically integrating the two-dimensional Boussinesq equation [see, e.g., *Verruijt*, 1982]

$$\frac{\partial h}{\partial t} = \frac{1}{\varphi} \left[\frac{\partial}{\partial x} \left(kh \frac{\partial h}{\partial x} \right) + \frac{\partial}{\partial y} \left(kh \frac{\partial h}{\partial y} \right) \right] \quad (7)$$

in a locally isotropic medium (i.e., k is a scalar) with either homogeneous (i.e., k is constant in space) or heterogeneous regional grid properties using a Crank-Nicholson implicit finite difference scheme. A 10 by 10 m mesh was applied with 10 min time increments. When a sloping impervious layer was employed during the analysis, the average slope did not exceed 1:100 in order to ensure the validity of the Dupuit assumption [*Verruijt*, 1982].

The prescribed model parameters for the rectangularly

shaped aquifer and for the small watershed are displayed in Table 1. The assigned saturated hydraulic conductivity values are typical of a sedimentary material consisting of poorly sorted sand [see, e.g., *Domenico and Schwartz*, 1998, p. 39].

In the heterogeneous case a conductivity value was assigned to each cell in the model at random following a lognormal distribution as generally observed in aquifers [see, e.g., *Law*, 1944; *Nielsen et al.*, 1973]. In cases where the conductivities are intended to display high spatial autocorrelation in certain directions among cells (i.e., macroscopic anisotropy) the same values of the conductivities were used as in the simple (i.e., no preferred directions for k) heterogeneous case, except that the conductivity values were rearranged among the cells. The intent was to check the ability of the technique to quantify effective properties in the presence of high spatial autocorrelation of hydraulic conductivities as often observed in aquifers. For example, during sedimentation processes, certain directions (often alongside an ancient river bed) exhibit high spatial autocorrelation of the physical parameters because of interconnected elongated fluvial channel-fill bodies [e.g., *Fogg*, 1986].

The simulations were initiated with saturated aquifers. For both aquifers the water surface was set to zero in the channel at all times, representing a fully penetrating stream. Figure 2 shows the geometry and the location of the streams in the synthetic watershed case.

The model simulated the first 100 days of drawdown following saturation of the unconfined aquifers. To make certain that the numerical model worked correctly, the analytical solutions of (1) were compared to the numerical solution of (7) for the rectangular aquifer with constant k (see Figure 3) described in Table 1 as case a (see *Hornberger et al.* [1970] for a similar comparison). The two solutions overlap, except in the region corresponding to the transition in the types (from short- to long-time) of the analytical solutions. This is because the analytical long-time solution is strictly valid only asymptotically, and also, it requires an inverse beta function describing the initial water table [*Polubarinova-Kochina*, 1962, p. 516]. The

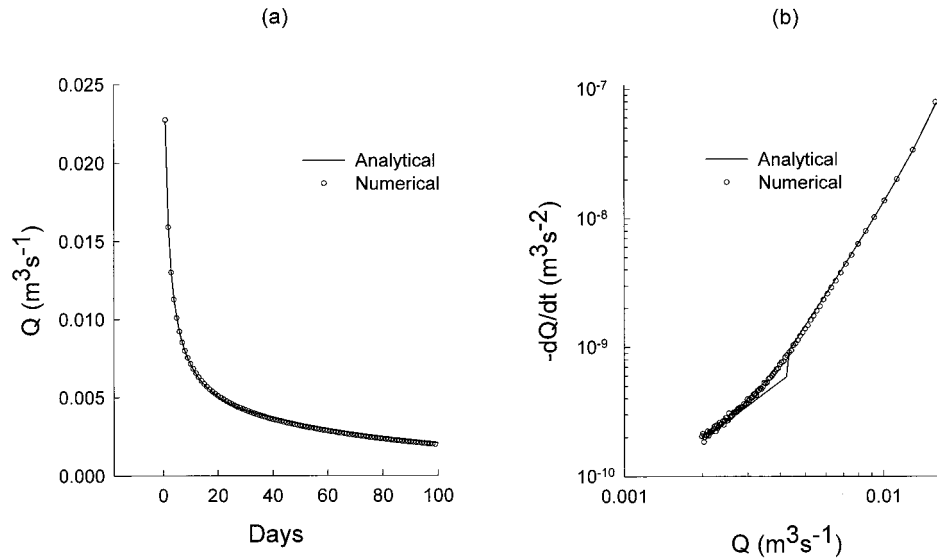


Figure 3. Comparison of the analytical and numerical solutions of the Boussinesq equation for the rectangular aquifer with constant saturated hydraulic conductivity and horizontal impervious layer: (a) Groundwater discharge through time and (b) time rate of change in discharge versus magnitude of discharge.

spatial distribution of the saturated hydraulic conductivities (i.e., heterogeneous case) for the rectangular region (cases b and c in Table 1, respectively), as well as the histogram of the conductivity values, are presented in Figure 4. The same are displayed in Figure 5 for the small synthetic catchment. The elevation of the sloping impervious layer for the two types of aquifer (cases d and e, respectively) is presented in Figure 6.

The numerical simulation results for 100 days of drought recession ($\log(-dQ/dt)$ versus $\log(Q)$) are given in Figure 7

for the rectangular aquifer and in Figure 8 for the synthetic catchment. As can be seen in Figures 7 and 8, two straight lines with slopes 3 (short-time solution) and 1.5 (long-time solution) can be fit to the graphs in each case with a relatively wide transition range between them. Because of the presence of this broad transition zone, the fit of the straight lines is somewhat arbitrary since the end of the short-time solution range, and similarly, the start of the long-time solution range is not well defined. The fitted equations are listed in Table 2. The esti-

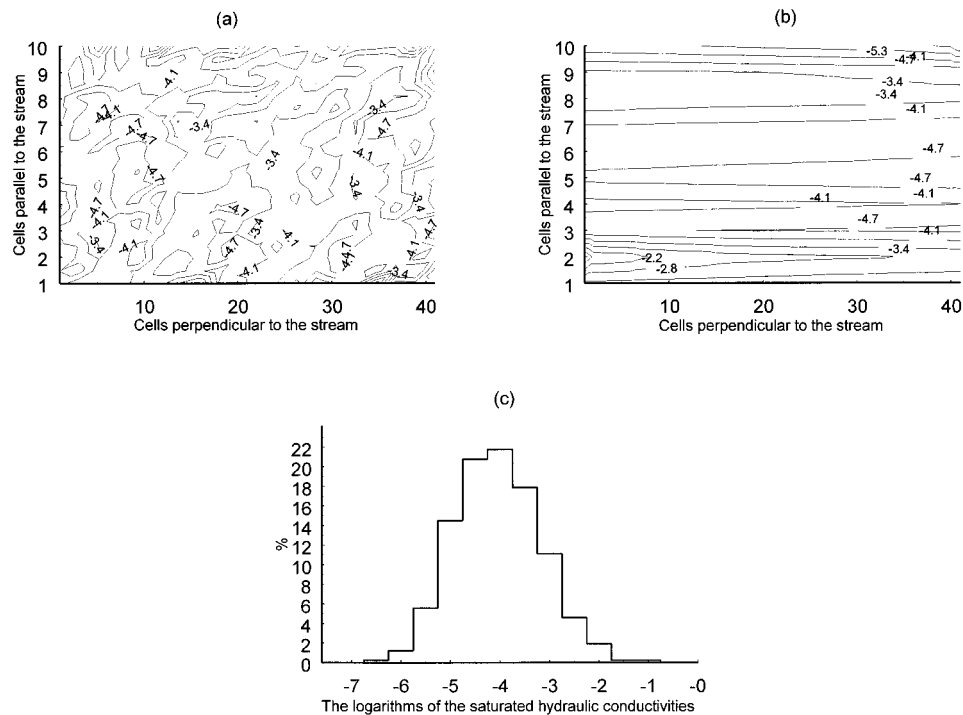


Figure 4. The spatial distribution of the saturated hydraulic conductivities (their 10 base logarithms are shown) (a) without and (b) with preferred directions in the rectangular aquifer case, as well as (c) their histogram. Cell dimensions are 10 by 10 m.

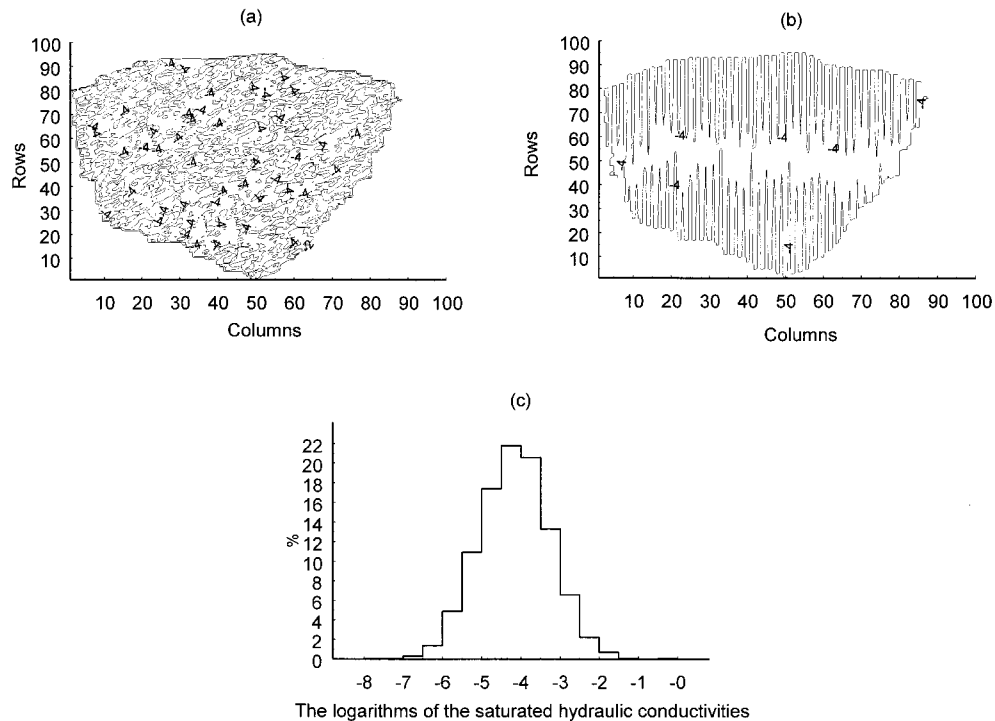


Figure 5. The spatial distribution of the saturated hydraulic conductivities (their 10 base logarithms are shown) (a) without and (b) with preferred directions in the synthetic catchment case, as well as (c) their histogram. Cell dimensions are 10 by 10 m.

mated hydraulic conductivity (k_{est}) and the estimated depth of the aquifer (D_{est}) are obtained using the fitted constants a_1 and a_2 (see Table 1 for the resulting estimated values).

Table 2 also displays the accuracy of the estimated parameters. We note that in the most ideal case (case a: constant k , horizontal impervious layer) the relative absolute error (i.e.,

the σ value) is $\sim 25\%$ for k and 10% for D . This might be due in part to (1) uncertainties in the curve fitting procedure, (2) the nonlinear nature of the equations involved, and (3) the numerical model itself. However, the accuracy of the estimated values does not deteriorate with increasing complexity of the aquifer.

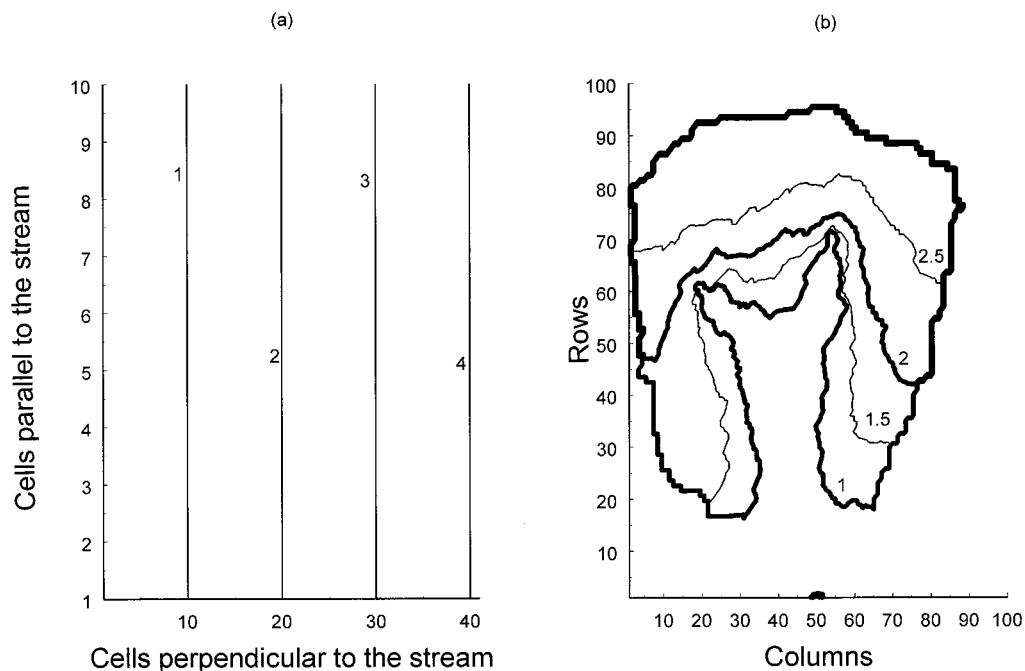


Figure 6. The elevation (meters above stream level) of the sloping impervious layer for (a) the rectangular aquifer and for (b) the synthetic watershed. Cell dimensions are 10 by 10 m.

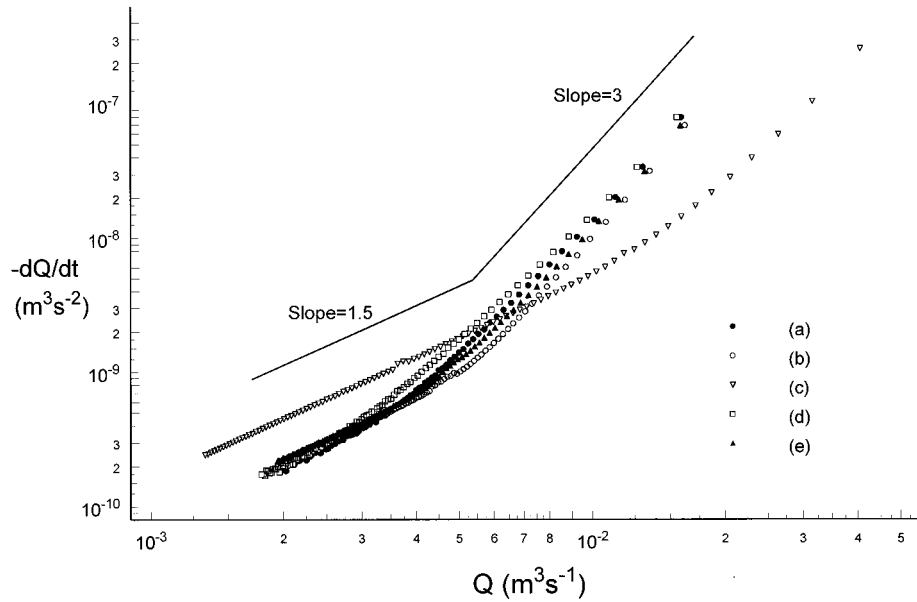


Figure 7. The time rate of change in discharge versus magnitude of discharge obtained from the numerical solution of the two-dimensional Boussinesq equation for the rectangular aquifer. The cases are a, constant saturated hydraulic conductivity k ; b, spatially variable k without preferred directions; c, spatially variable k with preferred directions; d, constant k with sloping impervious layer; and e, spatially variable k with sloping impervious layer.

As one would expect, the estimated effective value of the catchment-scale saturated hydraulic conductivity varies in accordance to the spatial distribution of k . Note that between cases b and c the only difference is in the spatial distribution of the conductivity values since the distribution function itself is the same lognormal distribution (see Table 1) with the same parameters in both cases. While the estimated conductivity

values in the heterogeneous cases (b, d, and e) with no preferred directions in the layering are much closer to the geometric mean [in accordance with Domenico and Schwartz, 1998, p. 43] of the lognormal distributions, the estimated hydraulic conductivity value in the rectangular aquifer case, where the layering is parallel to the groundwater flow, is closer to the arithmetic mean [Maidment, 1993, p. 6.11]. A similar

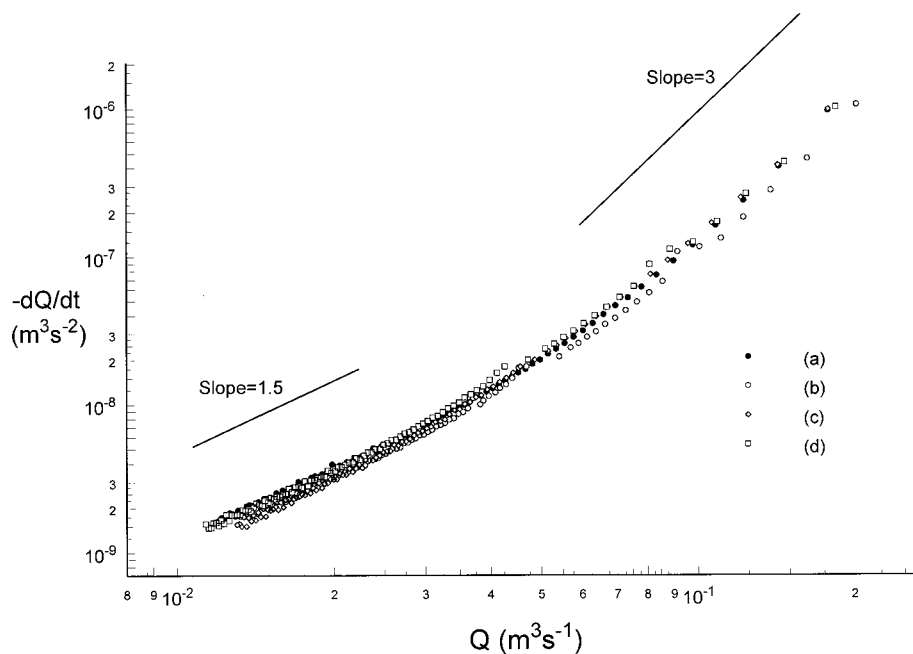


Figure 8. The time rate of change in discharge versus magnitude of discharge obtained from the numerical solution of the two-dimensional Boussinesq equation for the synthetic catchment. The cases are a, constant saturated hydraulic conductivity k ; b, spatially variable k without preferred directions; c, spatially variable k with preferred directions; and d, spatially variable k with sloping impervious layer.

Table 2. The Best-Fit Equations for the Short- ($dQ/dt = -a_1Q^3$) and Long-Time ($dQ/dt = -a_2Q^{1.5}$) Numerical Solutions in Figures 7 and 8 Plus the Relative Absolute Errors for the Saturated Hydraulic Conductivity k and the Mean Aquifer Depth D Estimates

| | Rectangularly Shaped Aquifer | Synthetic Watershed |
|--|--|--|
| Constant k | $-1.17 \times 10^{-2}Q^3$, $\sigma_k = 9$, $-2.22 \times 10^{-6}Q^{1.5}$, and $\sigma_D = 4$ | $-1.35 \times 10^{-4}Q^3$, $\sigma_k = 40$, $-1.27 \times 10^{-6}Q^{1.5}$, and $\sigma_D = 14$ |
| Spatially variable k | $-8.33 \times 10^{-3}Q^3$, $\sigma_k = 51$, $-2.48 \times 10^{-6}Q^{1.5}$, and $\sigma_D = 0$ | $-1.07 \times 10^{-4}Q^3$, $\sigma_k = 32$, $-1.13 \times 10^{-6}Q^{1.5}$, and $\sigma_D = 0$ |
| Spatially variable k with preferred directions | $-4.07 \times 10^{-3}Q^3$, $\sigma_D = 20$, and $-4.99 \times 10^{-6}Q^{1.5}$ | $-1.43 \times 10^{-4}Q^3$, $\sigma_D = 5$, and $-1.05 \times 10^{-6}Q^{1.5}$ |
| Constant k with sloping impervious layer | $-1.42 \times 10^{-2}Q^3$, $\sigma_k = 30$, $-2.30 \times 10^{-6}Q^{1.5}$, and $\sigma_D = 10$ | not investigated |
| Spatially variable k with sloping impervious layer | $-1.01 \times 10^{-2}Q^3$, $\sigma_k = 58$, $-2.54 \times 10^{-6}Q^{1.5}$, and $\sigma_D = 15$ | $-1.40 \times 10^{-4}Q^3$, $\sigma_k = 19$, $-1.23 \times 10^{-6}Q^{1.5}$, and $\sigma_D = 8$ |

Relative absolute errors are in percent; $\sigma_k = |k_{\text{est}} - k_{\text{mod}}|k_{\text{mod}}^{-1}$, $\sigma_D = |D_{\text{est}} - D|D^{-1}$; the subscript mod designates the modulus.

shift in the estimated conductivity value cannot be observed in the synthetic watershed case because there the layering is parallel in some parts, while in others it is perpendicular to the groundwater flow.

3. Summary

We explored the performance of the *Brutsaert-Nieber* [1977] recession flow analysis for estimating the catchment-scale saturated hydraulic conductivity and the mean aquifer depth by means of numerical simulation. The application of a numerical model made it possible to have control over the parameters to be estimated by the recession flow technique and to compare the prescribed values with their estimates. Such a comparison is generally not possible when the technique is applied in the case of real watersheds because of the obvious heterogeneity in the aquifer.

The effect of complex geometry, a gently sloping impervious layer, and spatially variable saturated hydraulic conductivities on the accuracy of the estimated catchment-scale parameters was investigated. It was found that the accuracy of the estimated parameters was not affected by the growing complexity of the synthetic aquifer employed in the model.

On the basis of our numerical model experiment the investigated recession flow technique proved to be reliable to estimate the catchment-scale saturated hydraulic conductivity k and the mean aquifer depth D . If the conditions required for the applicability of the Boussinesq equation are met, the technique is expected to provide reliable estimates of k and D in practical applications.

Acknowledgments. The authors gratefully acknowledge funding from the Johns Hopkins EPA grant on climate change and human health. This publication was made possible by grant 5 P42 ES04699 from the National Institute of Environmental Health Sciences, NIH, with funding provided by EPA. The authors are also grateful to the reviewers whose comments led to important revisions.

References

- Anderson, M. P., and W. M. Woessner, *Applied Groundwater Modeling*, p. 381, Academic, San Diego, 1992.
- Boussinesq, J., Sur un mode simple d'écoulement des nappes d'eau d'infiltration a lit horizontal, avec rebord vertical tout autour lorsqu'une partie de ce rebord est enlevée depuis la surface jusqu'au fond, *C. R. Acad. Sci.*, 137, 5–11, 1903.
- Brutsaert, W., and J. L. Nieber, Regionalized drought flow hydrographs from a mature glaciated plateau, *Water Resour. Res.*, 13, 637–643, 1977.
- Domenico, P. A., and F. W. Schwartz, *Physical and Chemical Hydrogeology*, 2nd ed., pp. 506, John Wiley, New York, 1998.
- Fogg, G. E., Groundwater flow and sand body interconnectedness in a thick, multiple aquifer system, *Water Resour. Res.*, 22, 679–694, 1986.
- Hornberger, G. M., J. Ebert, and I. Remson, Numerical solution of the Boussinesq equation for aquifer-stream interaction, *Water Resour. Res.*, 6, 601–608, 1970.
- Horton, R. E., Erosion development on streams and their drainage basins: Hydrophysical approach to quantitative morphology, *Geol. Soc. Am. Bull.*, 56, 275–370, 1945.
- Law, J., A statistical approach to the interstitial heterogeneity of sand reservoirs, *Trans. Am. Inst. Min. Metall. Pet. Eng.*, 155, 202–222, 1944.
- Maidment, D. R. (Ed), *Handbook of Hydrology*, McGraw-Hill, New York, 1993.
- Nielsen, D. R., J. W. Biggar, and K. T. Erh, Spatial variability of field-measured soil-water properties, *Hilgarda*, 42, 215–259, 1973.
- Polubarinova-Kochina, P. Y., *Theory of Groundwater Movement*, pp. 613, Princeton Univ. Press, Princeton, N. J., 1962.
- Troch, P. A., F. P. de Troch, and W. Brutsaert, Effective water table depth to describe initial conditions prior to storm rainfall in humid regions, *Water Resour. Res.*, 29, 427–434, 1993.
- Verruijt, A., *Theory of Groundwater Flow*, pp. 144, MacMillan, Indianapolis, Indiana, 1982.

J. D. Albertson, Department of Environmental Sciences, University of Virginia, Charlottesville, VA 22903.

M. B. Parlange, Department of Geography and Environmental Engineering, Johns Hopkins University, Baltimore, MD 21218–2686.

Jozsef Szilagyi, Conservation and Survey Division, University of Nebraska, Lincoln, NE 68588-0517. (e-mail: jszilagy@unlinfo.unl.edu.)

(Received August 21, 1997; revised March 13, 1998; accepted March 24, 1998.)

